Analysis of interfacial interaction in UHPFRC-strengthened reinforced concrete beams

IOP Conf. Series: Materials Science and Engineering **596** (2019) 012024 doi:10.1088/1757-899X/596/1/012024

Analysis of interfacial interaction in UHPFRC-strengthened reinforced concrete beams

C Zanuy, G S D Ulzurrun and I M Díaz

Dept. Continuum Mechanics & Structures, Universidad Politécnica de Madrid, ETS Ingenieros de Caminos, 28040 Madrid, Spain

E-mail: carlos.zanuy@upm.es, https://orcid.org/0000-0001-9044-8666

Abstract. The behaviour and failure mode of reinforced concrete elements strengthened with a thin tensile layer of ultra-high performance fiber-reinforced concrete (UHPFRC) is governed by the interface interaction between the UHPFRC and conventional concrete. In order to analyze the relative displacements at the interface and its influence on the crack pattern evolution and monolithic response, digital image correlation (DIC) has been used in this contribution. With the help of DIC, the distinct stages of the behaviour of UHPFRC-strengthened beams have been correlated with the crack formation and development. Special attention has been paid to the progressive debonding due to the strain incompatibility between UHPFRC and conventional concrete when cracks develop. It is shown that the utilization of the capacity of the UHPFRC can be achieved from a certain thickness of the strengthening layer for shear-critical elements, thereby providing a gain of shear strength and ductility. In contrast, a thinner UHPFRC layer has been more beneficial for flexure-critical elements.

1. Introduction

The use of ultra-high performance fiber reinforced concrete (UHPFRC) to strengthen concrete structures with a thin layer at the tensile part has shown to be an effective structural solution [1]. In such composite members, the interaction between the UHPFRC and reinforced concrete components is responsible for the monolithic behaviour and the failure mode [2]. UHPFRC and conventional concrete have a distinct fundamental behaviour, especially in tension: while conventional concrete cracks without appreciable post-peak softening capacity, UHPFRC is able to develop a strain-hardening stage before the formation of macro-cracks and a significant softening stage thereafter [3]. Progressive relative displacements (tangential slip and normal debonding) along the UHPFRC-conventional concrete interface develop as each layer enters a distinct stage, which characterizes the failure mode of the composite member [4]. The efficiency of composite structures (including steel-concrete, FRP-concrete, FRP-steel, etc) typically relies on the interface behaviour.

The present contribution aims at analyzing the influence of the global response of UHPFRC-strengthened reinforced concrete beams paying attention at the evolution of the interface between both layers. Results of quasi-static tests are presented and digital image correlation (DIC) technique is employed to follow the relative interface displacements and crack pattern development.

2. Experimental approach

2.1. Description of test configuration

Six beams have beam tested under quasi-static loading to failure in a three-point bending configuration as represented in Figure 1. The external dimensions (2000 x 125 x 250 mm) and longitudinal reinforcement (2Φ16 at bottom and top) were the same for all specimens. Three beams were designed without stirrups (referred to as RC-series) and three other beams with Φ8 stirrups at 15 cm spacing (referred to as RCS-series), thereby covering shear- (RC-series) and flexure-critical members (RCS-series). Reference specimens RC and RCS contained no UHPFRC strengthening layer, while specimens xxx-U35 and xxx-U55 included a UHPFRC layer at the tensile face of 35 and 55 mm thickness, respectively. The longitudinal reinforcement and the stirrups were partially embedded by the UHPFRC layer when its thickness was 55 mm, but not when the thickness was 35 mm. It is noted that some authors [1] have recommended the introduction of additional longitudinal bars within the UHPFRC layer and an eventually higher member height in order to increase the member's resistance instead of just repairing it. Nevertheless, additional reinforcement and increase of section height have not been considered in the present research in order to allow direct comparison between strengthened and conventional beams.

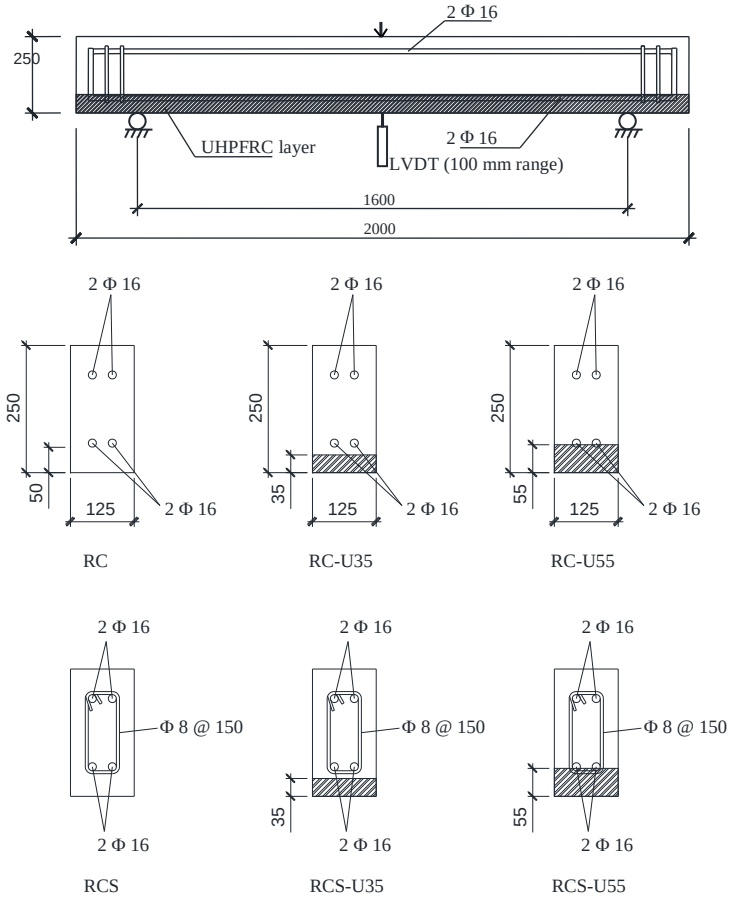

Figure 1. Test configuration and dimensions (in mm).

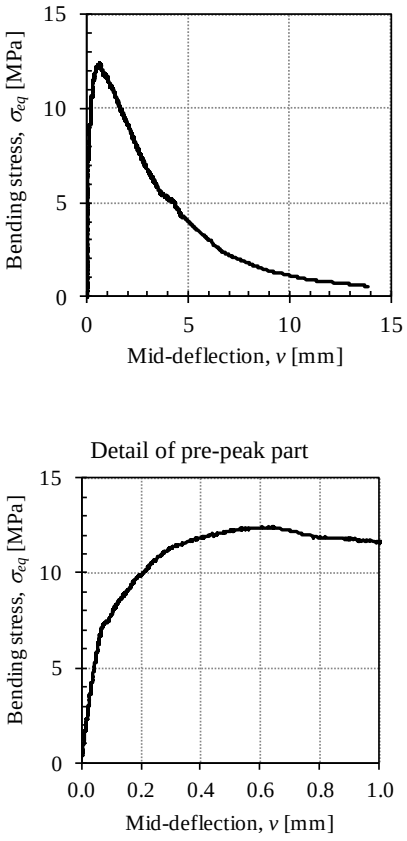

Figure 2. Example of material test (4-point bending on 500 x 100 x 100 mm prisms).

The specimens were manufactured and tested at the Laboratory of Structures of the Technical University of Madrid (UPM), Spain. The conventional concrete was supplied by a local contractor. The average cylinder strength at testing age was 41 MPa and the maximum aggregate size was 12 mm. For the specimens to be strengthened with UHPFRC, the total height was not concreted, i.e. the height of 35 or 55 mm was left empty instead of concreting and demolishing. In the later case, the beams were manufactured upside down. The upper surface of the RC layer was not levelled nor conditioned, so that the roughness of the interface was the natural surface of concrete. Before pouring the self-

compacting UHPFRC, the surface was washed, slightly wire brushed to remove loose material, and kept moist. The age of the conventional concrete was 15 months when the UHPFRC layer was manufactured. The UHPFRC was mixed in the laboratory from CRC premix kindly supplied by Hi-Con A/S (Denmark). The dry-mortar premix was mixed with the water and the fibers following the instructions of the supplier. A 2% volumetric amount of short straight steel fibers (12 mm length, 0.4 mm diameter) was used. The average cubic compressive strength at testing age (2 months after manufacturing) was 135 MPa. Flexural tests on prismatic specimens were also carried out to check the tensile behaviour of the UHPFRC: strain-hardening could be observed by formation of microcracks and a noticeable pre-peak stage (e.g. see Figure 2).

The tests were carried out by applying a monotonic displacement on the top side of the midspan section with a hydraulic actuator at a rate of 0.02 mm/s. The applied load was measured with a built-in load cell. An LVDT of 100 mm range was used to measure the midspan deflection at the bottom side (refer to Figure 1). In addition, a speckle pattern was painted on the front side of specimens in order to take pictures for DIC post-processing of test results. The photographs were taken by a Nikon D90 camera with lens Nikon 18-200 mm f/3.5-5.6, taking pictures of 4288 x 2848 px resolution every 5 seconds (approx.).

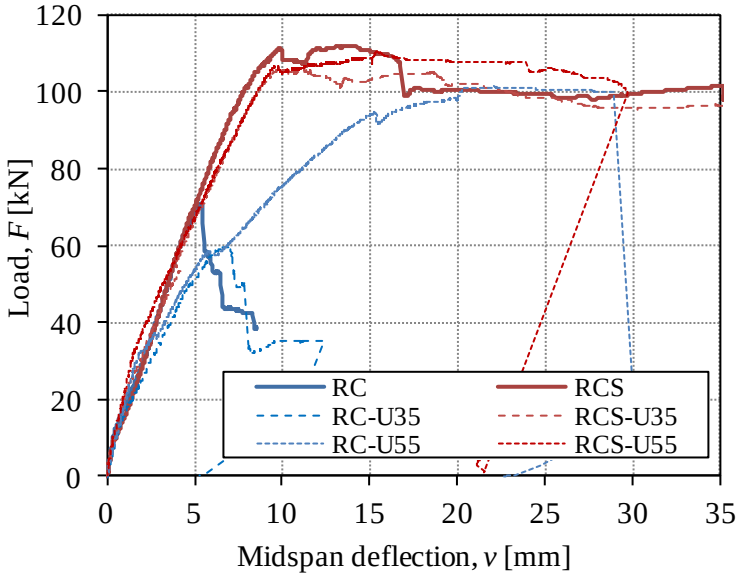

Figure 3. Load-midspan deflection of tested beams.

2.2. Test results

The behaviour of the specimens can be classified into two groups according to the failure mode: the beams without stirrups failed by shear and the beams with stirrups presented a flexural failure mode. The load-deflection curves of all tested specimens are represented in Figure 3. The crack patterns after failure are plotted in Figure 4. It has to be noted that cracks painted in red colour were developed before the tests started, while cracks formed during the tests are remarked in blue colour. Pre-test cracks were probably due to the shrinkage of the UHPFRC during the 2 months from manufacturing to testing. During that time, the beams had been supported horizontally on the laboratory floor in upside down position. As observed from red cracks in Figure 4, pre-test cracks included a longitudinal crack along the interface near the ends. For the beams with a 55 mm UHPFRC layer, the length of the interface crack was smaller than 10 cm, while for beams with a 35 mm thick layer, the length was around 25 cm, thereby entering in the span between supports. Moreover, some very thin transverse cracks were observed in both RC and UHPFRC layers close to the interface. For beams with a 35 mm UHPFRC thickness, those cracks (1 at midspan for RC-U35 and 2 away from the midspan for RCS-U35) crossed the whole height of the UHPFRC. For breams with a 55 mm UHPFRC thickness, only 1 transverse crack was observed at the UHPFRC, away from the midspan and not crossing fully its

thickness. In all cases, the largest crack opening of pre-test longitudinal and transverse cracks was 0.1 mm. This description of pre-test cracks can help in interpretation of test results.

The reference reinforced concrete beams RC and RCS presented shear and flexural failure, respectively. Test of beam RCS was stopped after a midspan deflection of 35 mm (span length/45) had been reached and some concrete spalling at compression zone started to occur.

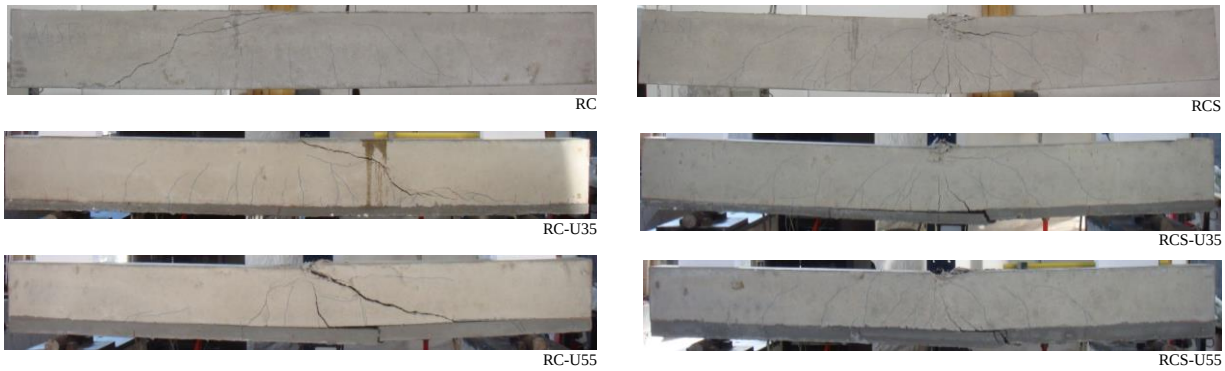

Figure 4. Crack pattern of tested beams after failure.

Composite specimens RC-U35 and RC-U55, without stirrups, developed shear failures. The influence of the thickness of the UHPFRC layer was quite significant, as RC-U35 showed a shear strength 15% smaller than the reference RC beam. In contrast, RC-U55 presented a 43% higher strength and was able to develop some pseudo-ductility. It is interesting to note that the initial stiffness of both RC-U35 and RC-U55 was not higher than that of the reference RC beam, which can be attributed to the effect of pre-test cracks crossing the UHPFRC layer which might avoid the full utilization of the pre-cracking and strain-hardening stages of the UHPFRC. This effect is further analyzed in section 3.3. From the crack pattern (Figure 4), it is also observable that the tensile capacity of the UHPFRC could be fully utilized by specimen RC-U55 but not by specimen RC-U35 (see the wide macro-crack crossing the UHPFRC layer in beam RC-U55 and the associated interface debonding, not developed by RC-U35).

Composite specimens RCS-U35 and RCS-U55, with stirrups, reached yielding of the longitudinal reinforcement and developed a significant plateau thereafter. They presented approximately the same loading capacity as the reference RCS beam. Test RCS-U35 was stopped after a midspan deflection of 35 mm with some spalling at the compression zone. The compression zone of test RCS-U55 exploited at a midspan deflection of 30 mm. This higher brittleness is due to the higher equivalent reinforcement ratio provided by both the tensile reinforcement and the 55 mm thick UHPFRC layer. Other authors also showed higher brittleness of flexure-critical composite members [5]. The initial stiffness of RCS-U35 and RCS-U55 was slightly higher than that of the reference RCS beam. In addition, a wide macro-crack accompanied by interface debonding developed and crossed the UHPFRC layer in both RCS-U35 and RCS-U55 specimens, showing high utilization of the UHPFRC layer.

Because interface debonding and crack development were responsible for the response of strengthened specimens, it is interesting to complete a deeper study of the interaction between the UHPFRC and conventional concrete layers. In this paper, the analysis is carried out with the help of DIC technique in section 3.

3. Analysis of results

3.1. DIC technique

Digital Image Correlation (DIC) is a robust and adaptable tool to analyze the deformed pattern of 2-D or 3-D problems from the photogrammetric follow-up of a speckle pattern painted on a solid. In the present contribution, 2-D DIC has been employed to study the in-plane deformational response of tested beams from a speckle pattern painted on the front side (2000 x 250 mm^2) and a camera placed perpendicularly in front of the midspan. The focal length of the lens was set to 24 mm. According to

the camera resolution (section 2.1), 1 px corresponded to 0.5 mm approx. The scale was provided with a line gauge on the beams' top side. The speckle pattern has consisted on randomly-painted black points of 1-3 mm size over a white background. GOM Correlate software [6] has been used for the DIC analysis, with a facet size of 30 px and a point distance of 20 px.

DIC can be more efficient than the installation of several transducers at different locations of the specimens in order to follow the evolution of e.g. displacements or strains. In the present contribution, the study has focused on the evolution of the UHPFRC-concrete interface and the crack pattern in correlation with the members' response and the stages of the load-displacement diagrams of Figure 3.

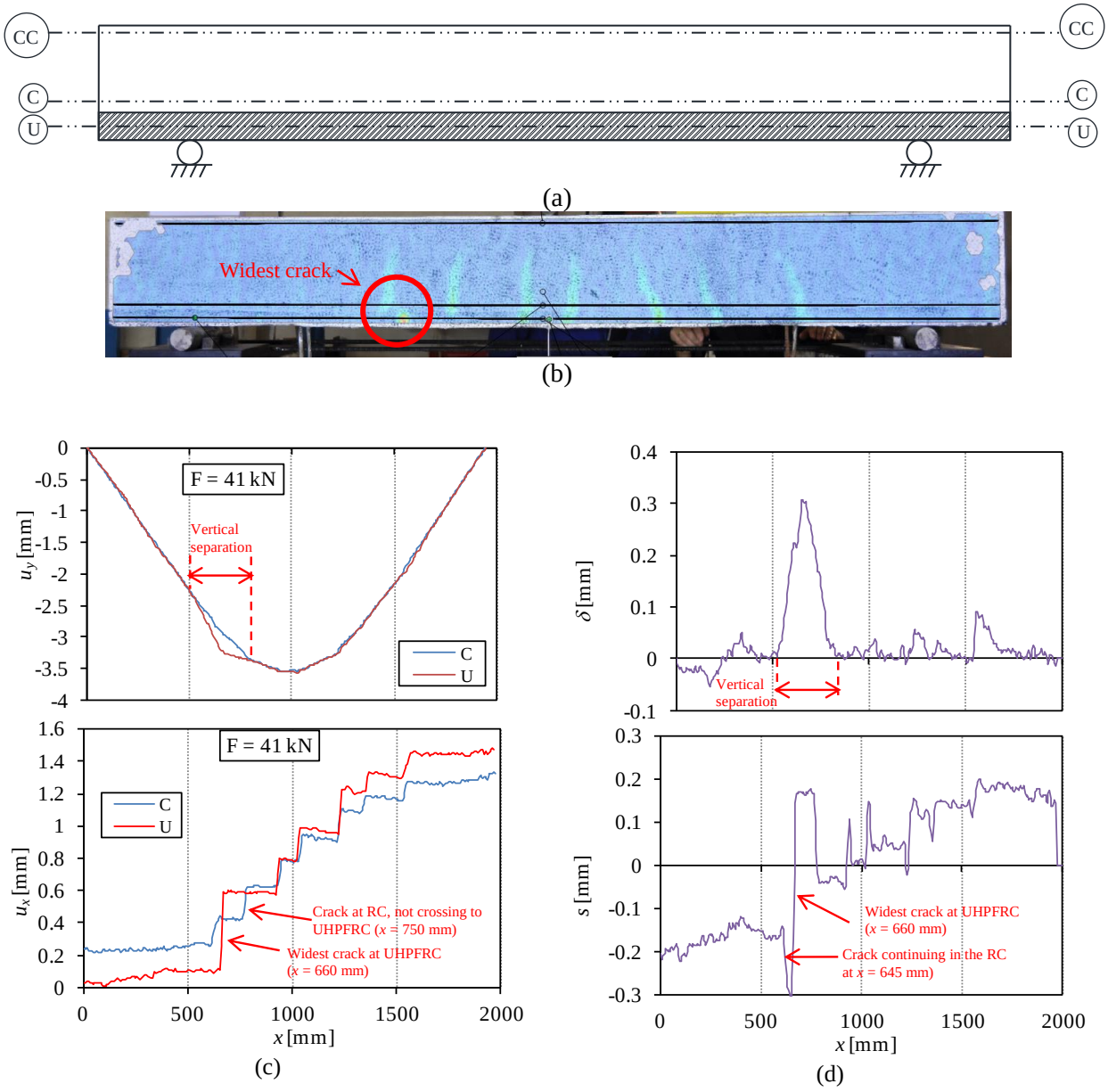

Figure 5. (a) Scheme of sections studied with DIC; (b) Field of horizontal strains of RCS-U35 under 41 kN; (c) horizontal and vertical displacements along UHPFRC and RC; (d) tangential slip and vertical separation along the interface.

The interface state can be characterized by the relative tangential slip and normal displacement between the UHPFRC and conventional concrete at the interface. Such relative displacements can be calculated by extracting the horizontal and vertical displacements along two horizontal sections at both

sides of the interface. Here, the sections at the centroid of the UHPFRC layer and 12 mm above the interface have been taken, which are denoted as *U* and *C* in Figure 5(a).

As an example to explain the methodology followed in this paper, the state of beam RCS-U35 under a load of 41 kN (service load level) is studied. The horizontal strain field is represented in Figure 5(b). Highly concentrated strains typically indicate cracks. The horizontal and vertical displacements along both sides of the interface are plotted in Figure 5(c). From the horizontal displacements (u_x), each vertical jump indicates the presence of a crack and the corresponding crack width can be calculated as the difference between the horizontal displacements at both sides. According to Figure 5(c), 6 cracks can be found along *U* and 7 cracks along *C*. There is one crack at x = 750 mm which is present in *C* but not in *U*, which can be confirmed from the picture in Figure 5(b). Moreover, the widest crack is placed at x = 660 mm and its width is 0.48 mm. The widest crack can also be found in Figure 5(b). Vertical displacements (u_y) in Figure 5(c) also provide relevant information, as the difference between u_y at *U* and *C* shows vertical debonding.

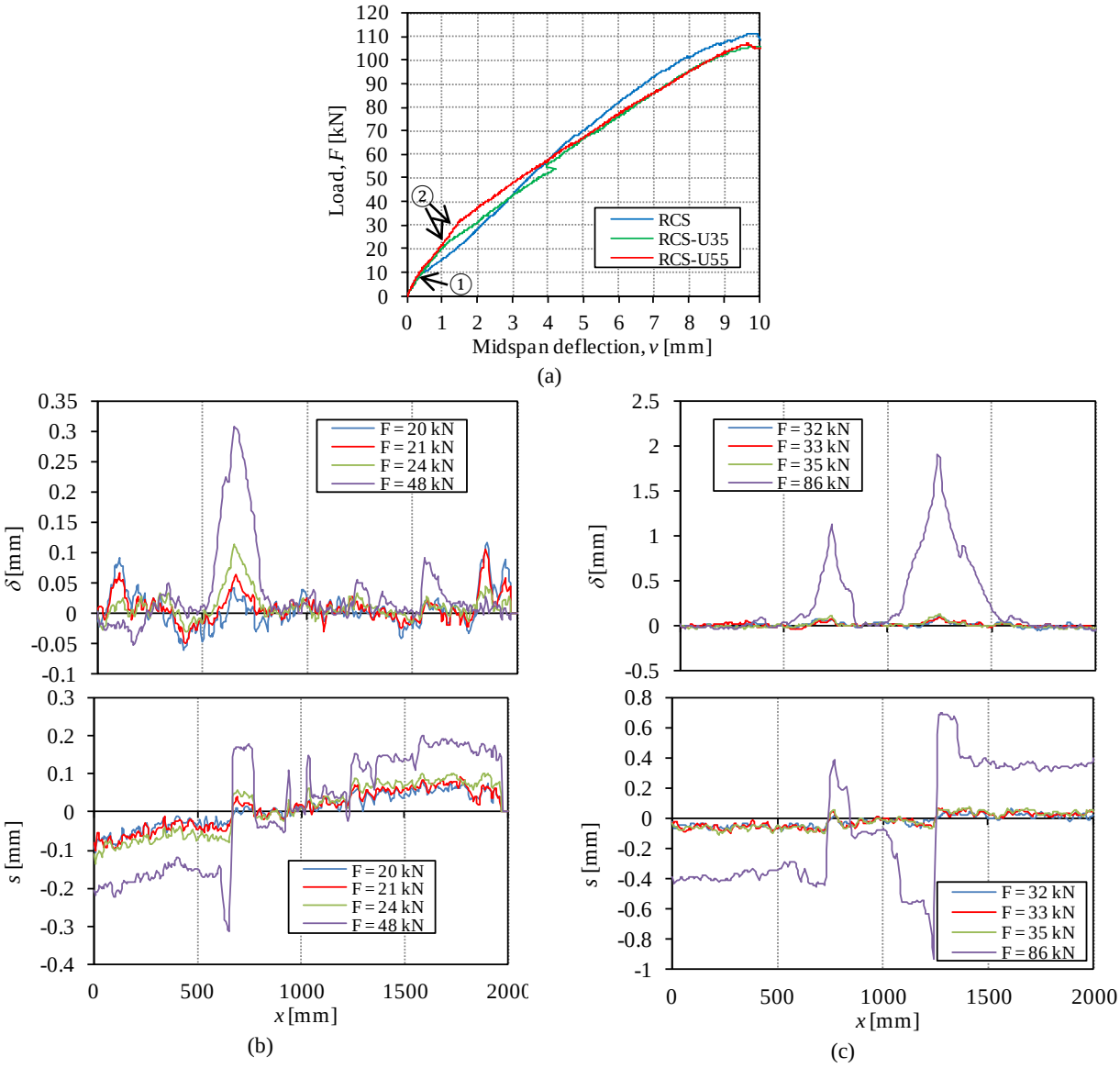

Figure 6. Analysis of RCS-series: (a) Detail of pre-peak part of load-deflection diagrams; (b) Interface relative displacements during pre-peak of RCS-U35; (c) Interface relative displacements during pre-peak of RCS-U55.

Relative displacements at the interface are represented in Figure 5(d). The tangential slip (s) is obtained by the difference between the horizontal displacements at U and C. Jumps of s represent cracks at either UHPFRC or conventional concrete and the value of the jump is the corresponding crack width. The detail of the analysis provides information like the fact that the widest crack at U (x = 660 mm, width = 0.48 mm) does not continue to C at the same position, but 15 mm to the left (x = 645 mm, width = 0.15 mm), which can be also observed by carefully looking at u_x in Figure 5(c) and the strain field in Figure 5(a). Analogously, the relative normal displacements at the interface (δ) are calculated by the difference of the vertical displacements at U and C and they can be used to study the vertical debonding. According to Figure 5(d), vertical separation produced by the widest crack at UHPFRC extends over a length of 300 mm and has a maximum value of 0.3 mm. Smaller separation also exists around each crack. The curvature of the deflected shape (u_y) along U indicates negative bending of the UHPFRC layer in the zone where vertical debonding develops, which has been considered as other authors to explain the contribution of the strengthening layer [4].

From the variables explained above, a detailed analysis of the interface state can be carried out. In the following sections, the evolution of the interface is studied in correlation with the global response of tested composite members.

3.2. Analysis of flexure-critical beams

The composite specimens that contained stirrups (RCS-U35 and RCS-U55) failed in a similar way as the reference reinforced concrete beam RCS, but with a smaller ductility due to compression zone destruction. The DIC technique is employed to analyze the crack pattern evolution and the behaviour of the interface in correlation with the load-deflection diagram.

The pre-peak part of the load-deflection diagram of RCS-series is represented in Figure 6(a). Relative displacements at the interface between UHPFRC and conventional concrete are displayed in Figure 6(b) and (c) for different load levels of RCS-U35 and RCS-U55, respectively. The first load level represented in Figure 6(b) and (c) is the load below which cracks are not detected with the DIC.

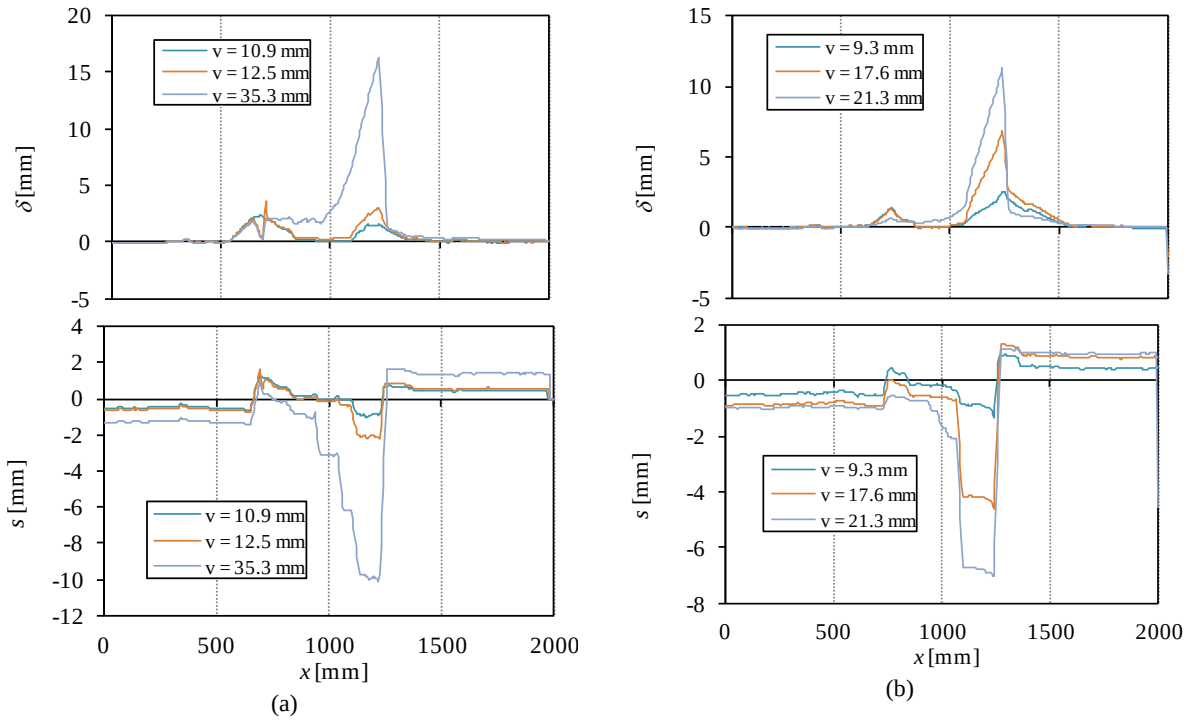

Figure 7. Interface relative displacements during post-peak: (a) RCS-U35; (b) RCS-U55.

In the initial stage of the load deflection diagram, two key points can be distinguished. Point ① in the RCS beam represents the cracking load, i.e. the tensile strength of conventional concrete is reached at the bottom of the beam. The load is around 10 kN. At that load level, a slight change of stiffness can

be also observed in the load deflection diagram of RCS-U35 and RCS-U55, but the bottom of the beam is of UHPFRC. Because Figure 6(b) and (c) shows that no cracks open until 21 kN and 33 kN for RCS-U35 and RCS-U55, respectively, point ① indicates the matrix microcracking of the UHPFRC and the beginning of the strain hardening stage. Indeed, from point ①, the response of UHPFRC-strengthened beams is stiffer than that of RCS beam.

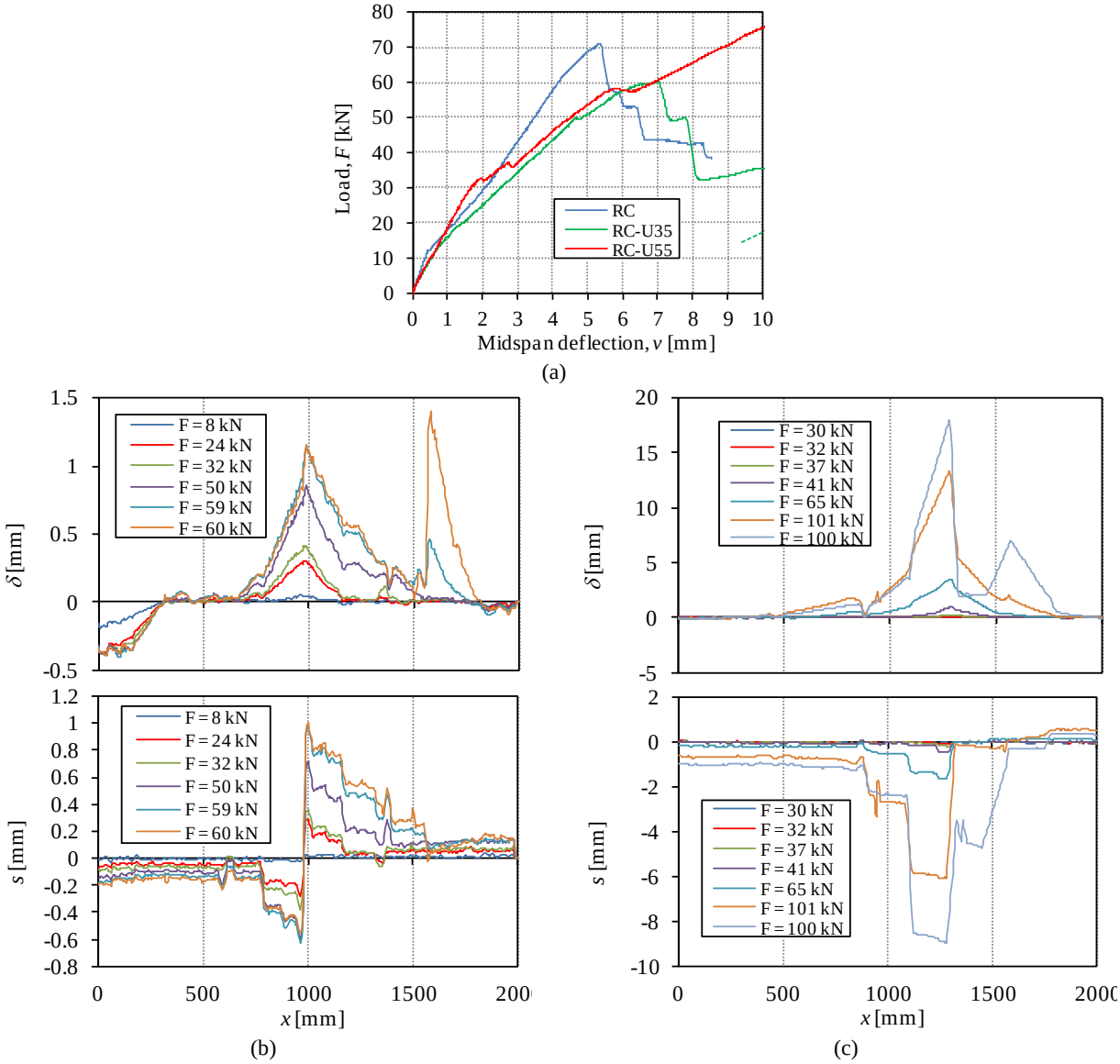

Figure 8. Analysis of RC-series: (a) Detail of load-deflection diagrams; (b) Interface relative displacements of RC-U35; (c) Interface relative displacements of RC-U55.

A second characteristic point ② in the response of UHPFRC-strengthened specimens shows decrease of stiffness. The load level of point ② (21 kN and 33 kN for RCS-U35 and RCS-U55, respectively) corresponds with the detection of the first macro-crack in the UHPFRC, as noted from the jumps detected in the relative displacements at the interface. For increasing load levels, more macro-cracks develop in the UHPFRC until a number of 6 macro-cracks for RCS-U35 and 2 macro-cracks for RCS-U55. Additional cracks form progressively in the conventional concrete layer (e.g. refer to Figure 5). Accompanying the formation of cracks, the progression of vertical debonding can be followed by analyzing the relative vertical displacement at the interface. It can be observed that a longer debonding zone is obtained for larger crack widths, which seems logical as vertical separation is a result of the incompatibility of strains produced by cracks. In addition, crack widths have been

significantly smaller in the specimen with 35 mm thick UHPFRC layer than that with 55 mm thickness, due to the higher number of cracks formed. The 2 cracks formed in specimen RCS-U55 had a considerable width in the pre-peak part of the test

The evolution of the relative displacements at the interface during post-peak stage is studied in Figure 7. Each curve is denoted by the midspan deflection of the specimen (v). At the yielding point, a shear plug was visible in the midspan zone of RCS-U35. The shear plug is characterized by two cracks with an inclination of 70-80º in the concrete zone, continuing across the UHPFRC with 2 macro-cracks. The largest crack width at the UHPFRC was around 2 mm at the peak load. Form that value, it then increased until one of the cracks reached 2.5-3.0 mm, when the UHPFRC layer divided into two parts. In spite of that, the beam was still able to carry loads without release. The test was stopped at a midspan deflection of 35 mm. The response of beam RCS-U55 was similar, but the lesser number of cracks resulted in a larger width of them, as their width was already 2.5 mm under the peak load and the UHPFRC layer divided into two parts at that load level. The specimen was able to continue carrying the load despite the breakage of the UHPFRC layer with the formation of a shear plug in the central region, until final failure of the compression zone.

From the above result, it has been observed how the UHPFRC layer has been able to provide carrying capacity even after its breakage during the post-peak stage, when a tied-arch mechanism seems to bridge the load. It is noted that the widest macro-cracks in the UHPFRC were not the pre-cracks formed by shrinkage prior to testing, i.e. in these tests pre-test cracks have not influenced the response of the beams.

3.3. Analysis of shear-critical beams

The composite specimens without stirrups (RC-U35 and RC-U55) failed by shear, as well as the reference reinforced concrete specimen RC. The evolution of those specimens is studied with the help of load-deflection curve and relative displacements at the interface, represented in Figure 8.

The first cracking load of the reference specimen RC was at a load of 10-11 kN. The behaviour of RC-U35 was dominated by the presence of a pre-crack crossing the UHPFRC layer at the midspan section (x = 1000 mm). From the relative displacements at the interface it is clear that the pre-crack has governed the global behaviour. On the one hand, vertical separation around that crack developed from the beginning of the test (see F = 8 kN in Figure 8(b)). On the other hand, the initial stiffness of specimen RC-U35 was smaller than that of the reference RC beam. The difference between measured midspan deflection of beams RC-U35 and RC (difference of green and blue curves in Figure 8(a)) has resulted equal to the relative vertical separation at the midspan obtained with the DIC (Figure 8(b)). It becomes apparent that the pre-crack has reduced the initial uncracked and strain-hardening stages. At a load of 24 kN, 2 additional macro-cracks opened at the UHPFRC, one of them at x = 1350 mm. From the later crack, significant vertical debonding extended to the midspan at a load of 50 kN. From that load, significant principal tensile strains in the web from the UHPFRC at x = 1350 mm to the compression zone at midspan were detected with the DIC. Finally, a diagonal crack opened at a load of 59 kN, which can be observed by the deformed shape obtained with the DIC along *CC* (refer to Figure 5(a)). The deformed shape along *U*, *C* and *CC* at a load of 59 kN are plotted in Figure 9, where it becomes clear not only the distortion produced by the diagonal crack, but also the significant debonding between the UHPFRC and the conventional concrete between x = 1000 mm and 1350 mm.

Regarding specimen RC-U55, its pre-cracks did not cross the UHPFRC layer. The initial stiffness was somewhat smaller than the reference RC beam, but higher than the one of RC-U35. The first change of stiffness of the load-deflection diagram was observed at a load of 32 kN. At that instant, the first macro-crack at UHPFRC was detected by the relative displacements at the interface at x = 1300 mm. That crack extended upwards in the conventional concrete at a different location (x = 1230 mm), thereby leading to beginning of vertical separation along the distance in-between. A second macro-crack at the UHPFRC opened at 38 kN at x = 880 mm. The peak of the load-deflection diagram at 41 kN was due to the formation of a shear plug in the centre of the reinforced concrete layer, with two cracks inclined 70-80º between x = 900 and 1100 mm. From 41 kN, vertical debonding was observable around the crack at x = 1300 mm and progressed until its crack width in the UHPFRC layer

reached 2-2.5 mm when the load was 58 kN. That point can be observed by a change of stiffness in the load-deflection curve and was characterized by the division of the UHPFRC into two parts from that section. Nevertheless, the load carrying capacity was not affected and the test load could be significantly increased as the interface progressively debonded to the right and the left of x = 1300 mm. The beam seemed to work as a tied arch with the longitudinal reinforcement bridging the stresses at the point of the macro-crack at UHPFRC. Simultaneously the cracks of the shear plug progressively opened further. The peak load was reached when the compression zone at midspan started to spall but a plateau could still be developed from a deflection of 20 mm to 29 mm, when a diagonal crack extended fully from the compression zone at midspan to the debonded UHPFRC-conventional concrete interface. The UHPFRC with 55 mm thickness has provided an additional load carrying mechanism and pseudo-ductility with respect to the reference RC beam that could not be achieved with the 35 mm thickness.

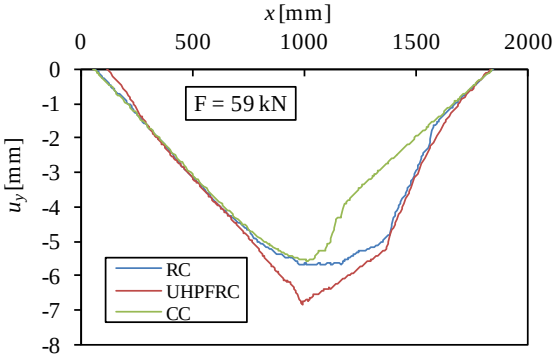

Figure 9. Deformed shape of beam RC-U35 under a load of 59 kN.

4. Conclusions

Digital Image Correlation (DIC) has been used in this research to study the interfacial behavior of UHPFRC-strengthened reinforced concrete beams. The study has focused on the identification of the different stages of the load-deflection diagrams by analyzing the crack pattern evolution and relative displacements between the UHPFRC and conventional concrete.

It can be concluded that DIC is a reliable technique to follow the horizontal slip and vertical separation at the interface, as well as the formation and widening of cracks. It has allowed following the evolution of the crack pattern including formation of shear plug at centre of beams, development of diagonal cracking, tangential slip and vertical debonding at the interface. It has been possible to detect the progressive vertical separation produced by the strain incompatibility due to different cracking at the UHPFRC and conventional concrete layers. For shear-critical beams, the properties of the UHPFRC have been utilized for the thicker UHPFRC layer, which has provided significant improvement of shear strength and ductility with respect to reference reinforced concrete beam. For flexure-critical beams, a better behaviour has been obtained with the thinner UHPFRC layer, as the compression zone is less sensitive to spalling.

Acknowledgement

The financial support provided by the Spanish ministry for economy and competitiveness (Project ID BIA2016-74960-R AEI/FEDER, UE) is gratefully acknowledged. The CRC pre-mix and fibers have been kindly provided by Hi-Con A/S (Denmark). Also thanks to “Fundación José Entrecanales Ibarra” for funding the PhD fellowship of the second author.

References

[1] Habel K, Denairé E and Brühwiler E 2006 *J Struct Eng* Structural response of elements combining ultrahigh-preformance fiber-reinforced concretes and reinforced concrete **132** 1793-1800.

[2] Noshiravani T and Brühwiler E 2013 *ACI Struct J* Experimental investigation on ultra-high-preformance fiber-reinforced concrete composite beams subjected to combined bending and shear **110** 251-61.

[3] Wille K, El-Tawil S and Naaman AE 2014 *Cem Concrete Comp* Properties of strain hardening ultra high performance fiber reinforced concrete under direct tensile loading **48** 53-66.
[4] Noshiravani T and Brühwiler E 2014 *J Struct Eng* Analytical model for predicting response and flexure-shear resistance of composite beams combining reinforced ultrahigh performance fiber-reinforced concrete and reinforced concrete **140** 1-10.
[5] Pimentel M and Nunes S 2016 *Proc. 4th Int. Symp. Ultra-High Performance Concrete and High Performance Materials (Kassel)* Experimental tests on RC beams reinforced with a UHPFRC layer failing in bending and shear (Kassel University Press) p 101-2.
[6] GOM. GOM Correlate 2018. Free version. 2018.